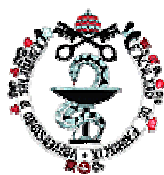**UNIVERSITY OF SALAMANCA**

FACULTY OF PHARMACY

DEPARTMENT OF MEDICINAL CHEMISTRY

DEVELOPMENT OF NEW ANTIMITOTIC AGENTS RELATED TO COMBRETASTATINS AND PHENSTATINS

DOCTORAL THESIS. English summary.

RAQUEL ÁLVAREZ LOZANO

June 2009

I. INTRODUCTION[1]

Cancer is a heterogeneous group of malignancies, characterized by an uncontrolled cell proliferation and tissue invasiveness. It is the second cause of mortality in developed countries, being the first one in Spain for male population.

Microtubules are the target of several anticancer drugs, due to their significant role in many cellular processes of paramount importance, such as mitosis, transport and cell motility. Microtubules are cylinders formed by protofilaments composed of α,β-tubulin heterodimers and show a dynamic instability (figure 1). Drugs interacting with tubulin interfere in microtubules dynamics, thus altering their functionality and producing fatal consequences on cells involved in division processes, which are more frequent in cancer cells.

---

[1] This english summary does not contain any figure or reference. Figures and references can be found in the spanish manuscript, which has the same chapters and sections than this summary.

At least five different sites for ligands are found in tubulin, those for structural GTP (exchangeable, E site, and non-exchangeable, N site), and those for antimitotic drugs: taxol, vinca alkaloids and colchicine sites. Taxol produces stable non-functional microtubules, vinca alkaloids produce aberrant polycyclic structures and colchicine site ligands produce depolymerization of microtubules (figure 2). Many types of natural and synthetic compounds have been described as colchicine-site ligands. They show, as common structural feature, two aromatic systems held together by a 0-4 atoms bridge (figure 3). Many of them also have a trimethoxyphenyl ring moiety, as it is the case of podophyllotoxin, MTC, combretastatin A-4, phenstatin and colchicine.

During the last few years, our research group has been working on some of these families (mostly phenstatins and combretastatins), having found several compounds displaying high potencies in the inhibition of tubulin polymerization (submicromolar range) and cytotoxicity against tumoral cell lines (nanomolar range).

I.1. SAR OF COMBRETASTATINS.

Combretastatins are a group of natural products first isolated by Pettit *et al.* from bark of *Combretum caffrum,* a tree from the tropical areas of Africa and India. Combretastatin A-4, which shows the highest cytotoxicity, has been taken as structural reference to establish structure-activity relationships. As shown in figure 4, a bridge between two aromatic rings is required, having some general characteristics: maintain a relative proximity between both rings (*Cis* disposition if the bridge is a double bond), non-coplanarity between rings and small substituents on the bridge (for example a five membered ring as bridge).

I.1.A. <u>Ring A modifications.</u>

Ring A (2,3,4- or 3,4,5-trimethoxyphenyl ring) seems to be almost essential for high cytotoxic and tubulin polymerization inhibitory effects. Their replacement always produces less potent compounds.

I.1.B. <u>Ring B modifications</u>.

Ring B of combretastatin A-4 (guaiacol) accepts many modifications. Although the suppression of the methoxy group at position 4 produces a potency decreas, positions 2 and 3 allow a higher degree of variability. Suppression of 3-OH, replacement by Br or NH_2 groups and other derivatives for increasing water solubility (phosphate,..), have produced compounds which maintain the cytotoxicity and TPI effects (figure 5). The phosphate (CA-4P) and the amino (AVE-8062) derivatives are now in clinical trials (phase I-II).

Replacement of ring B by smaller rings entails a potency loss. However, its replacement by bicyclic systems such as naphthalene or indole is not (figure 6).

I.1.C. <u>Bridge modifications</u>.

Distance between both aromatic rings is a determinant factor. Compounds with smaller bridge size (1 or 2 atoms) display higher potency than compounds with longer bridges (3 or 4 atoms). The presence of a *cis*-double bond also increases the potency over *trans* isomers, which also decreases when a more flexible hydrogenated bridge is present.

Two atoms bridges as part of a small cycle also maintain high TPI effect. Many examples of highly potent compounds, having pentagonal cycles as bridges, have been described. Also, the effect of the stereochemistry of the bridge on the activity has been studied for dioxolane derivatives (Figure 7).

I.1.D. <u>Other modifications</u>.

Other structural modifications directed at maintaining the *cisoid*-disposition of the two rings have been assayed. Recently, our group described macrocyclic derivatives (Figure 8), which maintain such a disposition by binding both rings through an additional bridge (spacer). These modifications have a detrimental effect on the activity of this class of compounds, but allow the study of their effect on the conformations adopted by combretastatins.

I.2. SAR OF PHENSTATINS.

Phenstatins are benzophenone derivatives, which were synthesized in order to study the effect of one carbon bridge on the activity of combretastatins. The study of this family was continued because these compounds showed highly potent antimitotic effects and higher water solubility, one of the main problems associated to combretastatins (figure 9).

In general, SAR of phenstatins are similar to those of combretastatins: a trimethoxyphenyl ring is required as ring A, both rings should be maintained in a *cis*-like disposition and a higher degree of variability is admitted for ring B. However, there are modifications that produce different effects on the activity of both families, such as the substitution of ring B by a 3-indolyl moiety.

The direct correlation between TPI effect and cytotoxicity is different in both families, being phenstatins, in general, more potent inhibitors of tubulin polymerization but less cytotoxic than their related combretastatins.

I.3. PHARMACOPHORE AND X-RAY STRUCTURES OF TUBULIN.

Recently, a pharmacophore composed of seven attachment points has been proposed from a selection of diverse compounds binding to the colchicine site of tubulin. These seven points are: three hydrogen bond acceptors (A1, A2, A3), a hydrogen bond donor (D1), two hydrophobic centres (H1, H2) and one flat group (R1) (figures 10a and 10b). The presence of an additional hydrogen bond acceptor on the bridge of phenstatins (the carbonyl group, corresponding to A3 of the pharmacophore) could explain their higher TPI potency in comparison to combretastatins (figure 11).

Although this pharmacophore can help to design new compounds, not all the colchicine site ligands fully agree with this model.

The X-ray structures of the tubulin complexes with podophyllotoxin and DAMA-colchicine, recently described by the group of Prof. Ravelli, are also of importance for the design of new ligands of the colchicine site. Although there is a great structural variability among the ligands at the colchicine site, due to the high protein plasticity, this new tool allows to analyze the activity results and to rationalize the effects of structural modifications on the activity.

II. PLANNING AND OBJECTIVES

The general objective of this research is the synthesis and evaluation of new antimitotic agents combining these structural features: a trimethoxyphenyl ring, a 5-indolyl moiety and an olefinic bridge.

II.1. OLEFINIC BRIDGE.

According to previous SAR on combretastatins and phenstatins, the latter display higher tubulin polymerization inhibitory potency when compared with combretastatins with similar substitution pattern. An explanation of this fact has been put forward by the addition of an extra binding element in the pharmacophore model, represented by a hydrogen bond acceptor site (A3), occupied by the carbonyl group of the bridge of phenstatins. However, this explanation is at odds with our recent finding that equally substituted 1,1,-diarylethenes (isocombretastatins) are better inhibitors of tubulin polymerization than phenstatins.

For this reason, we have planned the synthesis and evaluation of a representative number of isocombretastatins (1,1,-diarylethenes).

II.2. AR$_1$ RING: TRIMETHOXYPHENYL.

Although the 3,4,5-trimethoxyphenyl is considered necessary for high potency, we have found that a 2,3,4-trimethoxyphenyl system as ring A yields derivatives with selectivity against some cancer cell lines. Accordingly, both systems will be used for the synthesis of compounds in this work.

II.3. AR$_2$ RING: 5-INDOLYL DERIVATIVES.

Because indole systems have proved to be good substitutes of guaiacol as ring B in combretastatins and phenstatins, the *N*-methyl-5-indolyl system has been taken as a structural base for further modifications. Following this approach, also new benzimidazole and benzoxazole derivatives have been planned.

II.4. OBJECTIVES.

After this general planning for this Ph.D. work, the particular objectives to be addressed have been:

First objective: synthesis of 1,1-diarylethenes (isocombretastatins) combining trimethoxyphenyl moieties with phenyl rings having the best substitution patterns of combretastatins and phenstatins. The results from this work will show the effect of these variations on the activity of these related families.

Second objective: synthesis of isocombretastatins based on the 5-indolyl moiety as ring B, carrying substituents at the C-3 position. These derivatives are of interest because of the synthetic accessibility, structural variability (carboxaldehydes, hydromethyl, oximes, etc.), the possibility of improving water solubility and interaction with the protein.

Third objective: synthesis of combretastatins and phenstatins carrying the same indolyl modifications that proved of interest in the isocombretastatins. Among the planned modifications, the preparation of the benzimidazole and benzoxazole derivatives will also be considered.

Fourth objective: preparation of some macrocyclic derivatives containing the indole as ring B in order to also include the indolyl moiety in these analogues of combretastatins, recently described by our group.

Fifth objective: perform the inhibition of tubulin polymerization assays of all the synthesized derivatives and establish the SAR of combretastatins, phenstatin and/or isocombretastatins carrying the indolyl moiety.

III. METHODS AND RESULTS

III.1. SYNTHESIS OF NON-MACROCYCLIC COMPOUNDS.

As planned in the previous section, the compounds to be synthesized are: A) Isocombretastatins or 1,1-diarylethenes, B) Phenstatins or diarylketones (benzophenones), and C) Combretastatins or 1,2-diarylethenes (figure 12).

III.1.A. Synthesis of isocombretastatins.

In order to accomplish objectives 1 and 2 the synthesis of isocombretastatins was planned as follows (Scheme 1). The 1,1-diarylethenes can be obtained by olefination of the bridge of the corresponding benzophenones (phenstatins), which can be produced by oxidation of diarylmethanols. The coupling between an aryl organometallic derivative and the required aromatic aldehyde was chosen for the preparation of the diaryl methanols due to the defined regiochemistry produced during this process.

III.1.A.1. Starting materials.

Required materials for the synthesis of isocombretastatins are commercially available, except O-siloxy derivatives (**11** y **12**) of isovanillin (3-hydroxy-4-methoxybenzaldehyde) and *N*-methyl-5-bromoindole. These compounds were obtained by standard silylation (required trialkylsilyl chlorides in presence of triethylamine as a base) and *N*-alkylation of indole (base treatment in presence of phase transfer catalyst and alkyl iodide as alkylating agent) procedures (figures 13 and 14).

The obtained materials do not have acidic hydrogens, which can interfere in forthcoming reactions. The *N*-methyl on the indole nucleus is also of interest because of the increased inhibition of tubulin polymerization displayed by previous combretastatins and phenstatins carrying this structural element.

III.1.A.2. Synthesis of diarylmethanols.

Three related methods were used for the synthesis of alcoholic derivatives (figures 15a, b and c). In the case of 3,4,5-trimethoxyphenyl-aryl-methanols (**18**, **21** and **28**) the Grignard reagent from 5-bromo-3,4,5-trimethoxybenzene was reacted with the required arylaldehyde to introduce the ring B. In the case of 2,3,4-trimethoxyphenyl-aryl-methanols (**33**, **36** and **40**) the organometallic derivative was directly prepared by lithiation of 1,2,3-trimethoxybenzene, favoured by the coordination of the lithium with the adjacent oxygen atom, also followed by the addition of the required arylaldehyde.

Finally, for the synthesis of *N*-methyl-5-indolyl derivatives (**44** and **57**), 5-bromo-*N*-methylindole was selected because of the lower prize of the starting material and similar yields obtained in the synthesis. Metallation using two equivalents of the metallating agent, produced the 2,5-dimetallated-*N*-methyl-1*H*-indole, which yielded the expected 2,3,4- or 3,4,5-trimethoxyphenyl 5-indolyl methanols upon treatment with the corresponding trimethoxybenzaldehyde. Formation of the dianion of *N*-methyl-1H-indole, prevents the appearance of indoles bonded through the 2-position after transmetallation processes of the mono-metallated derivatives (scheme 2).

These procedures are adequate to obtain diarylmethanols in good yields (usually higher than 70% after chromatographic purification) to prepare the planned derivatives. The structures of obtained products, yields and the ^{1}H NMR chemical shift of the hydroxylated methyne signal are shown in table 1.

III.1.A.3. Synthesis of phenstatins.

The next step in the synthesis of isocombretastatins is the oxidation of diarylmethanols to diarylketones (phenstatins). PDC is the oxidizing agent usually employed to this purpose, but during the oxidation of diarylmethanols carrying the 2,3,4-trimethoxyphenyl moiety cleavage products were obtained, so that magnesium permanganate under phase transfer conditions was assayed. Because of the low yields produced by this procedure, PDC oxidation at lower temperature was successfully employed without cleavage reactions of 2,3,4-trimethoxyphenyl derivatives (**19**, **22**, **29**, **34**, **37**, **41**, **45** and **58**). Diarylketones of both families were thus produced (figure 16 and table 2) in enough amounts to proceed with the synthesis of isocombretastatins. Characteristic ^{1}H NMR signals are shown in figure 17 and table 2.

III.1.A.4. Synthesis of isocombretastatins.

The final step in the synthesis of isocombretastatins was a Wittig reaction. Wittig reaction produces olefins in good yields in the presence of methoxy, trialkylsiloxy and nitro groups such as those present in the planned isocombretastatins. Under standard conditions (treatment of triphenylmethylphosphonium iodide in THF with *n*BuLi at low temperature followed by addition of the diarylketone and spontaneous raise to room temperature) isocombretastins **20**, **24**, **31**, **35**, **38**, **42**, **47** and **59** were produced in 20-84% yield (figure 18 and table 3).

The shift difference between the two olefinic protons in ^{1}H NMR is characteristic for derivatives with 3,4,5-trimethoxyphenyl (0.05-0.007 ppm) and 2,3,4-trimethoxyphenyl (0.3-0.4) moieties.

III.1.A.5. Modifications of aromatic ring Ar₂.

Once the phenstatins and isocombretastatins were obtained, modifications of these products were undertaken. The 2,3,4- and 3,4,5-trimethoxyphenyl moieties were maintained, because, although not absolutely required, they produce compounds displaying higher potency than products lacking them. The modifications studied in this work were introduced at positions 3 of the phenyl ring and indolyl moiety.

III.1.A.5.1. Modifications of the phenyl rings.

<u>Reductions of the nitro groups to amino groups.</u>

This trivial reduction produced quantitative yields of **25** and **39**when carried out with Zinc in acetic acid. For the reduction of the nitrophenstatin to the known aminophenstatin (**23**), required for comparison of the assayed activities, Fe in methanol/water/acetic acid was used to avoid the simultaneous reduction of the bridge group. (Figures 19 and 20).

<u>Silyl ethers deprotection.</u>

Required deprotection of silyl ethers **29**, **31** and **42** to the corresponding phenols **30**, **32** and **43** was carried out under standard conditions TBAF in THF (figure 21).

III.1.A.5.2. Modifications at the position 3 of indole.

The indole nucleus appears as highly convenient for the synthesis of antimitotic agents, when combined with the 3,4,5-trimethoxyphenyl moiety, as discussed before. Furthermore, the indole facilitates the controlled introduction of substituents, specially at its 3-position, which is the best localization for the preparation of such derivatives. 3-Substituted indole phenstatins can be considered as rigidified analogues of 3,4-disubstituted fenstatins (Figure 22).

Electrophyllic formylation is the choice to easily introduce the small, reactive and versatile formyl group.

Formylations.

Once the *N*-methylindole isocombretastatins were obtained, formylations at 3-position were carried out by the Vilsmeier-Haack procedure, and the obtained compounds were used as starting materials for further modifications.

The formylation reaction using an excess of dimethylformamide in the presence of 1mmol/mmol of POCl$_3$, yielded mono- **40**, **60** and di-formylated **50**, **61** derivatives (Figure 23) after hydrolysis of intermediate products. The extent of diformylation decreases upon reduction of the reaction time.

The NMR data of these compounds fully agree with the proposed structures and clearly show the existence of both *Z,E*-diastereomers of the diformylated derivatives. The *Z*-isomer could be purified by crystallization and identified by nOe techniques.

The fenstatin 3-formyl derivative **46** was also prepared (Figure 24) to check the effect of formylation in both related families.

Reductions of the aldehydes.

The first choice to prepare new derivatives from the 3-formyl-indolyl-isocombretastatins was the reduction to 3-indolylmethanols, by means of metal hydride reductions. The NaBH$_4$/MeOH reduction produced the alcohols **51** and **62** as shown in figure 25.

Formation of oximes.

Oximes were prepared because they have the possibility of further interactions with the protein, by establishing additional hydrogen bonds, and their transformation in other potentially active derivatives, such as the acetoximes.

Similar transformations were previously carried out at the bridge of phenstatins, thus producing highly potent derivatives.

By standard procedures, the oximes **53** and **64** were prepared (Figure 26) as a mixture of *Z,E*-isomers. Although they could be chromatographycally separated, the purified compounds rapidly isomerize in solution to the equilibrium mixture.

<u>Formation of hydrazones.</u>

By the same reasoning and due to the structural similarities, the hydrazones **56** and **68** were prepared to be included in the SAR studies. By standard procedures, the hydrazones were obtained as non resolvable mixtures of *Z,E*-isomers (Figure 27). The double bond can also be reduced during the reaction. For compounds with a 2,3,4-trimethoxyphenyl, these are the only isolated products (**68Z** and **68E**).

<u>Treatment of oximes with acetic anhydride.</u>

The acetoximes were prepared by treatment of the oximes with acetic anhydride in pyridine, yielding complex mixtures. By chromatographic separation, the 3-carbonitriles **54** and **65** on the indole and the *Z,E*-mixtures, **55** and **67,** of acetoximes derived from isocombretastatins were isolated. In one case, the phenstatin with a 3-indolecarbonitrile **66** was produced, probably, due to the presence of small amounts of phenstatin in the isocombretastatin used as starting material (figure 28).

III.1.A.6. Bridge modification.

Bridge modification is detrimental for the activity of these types of antimitotics, unless small size substituents are used. In addition, the hydrogenation of combretastatins double bond produces a noticeable reduction of the cytotoxicity and inhibition of tubulin polymerization. But for isocombretastatins, the hydrogenation only produces a small geometry and size change, without modification of the degrees of freedom. The hydrogenation of isocombretastatins is, therefore, an easy and revealing modification to assay during SAR studies.

Reduction of the bridge olefin.

In order to check if the sp^2 hybridization of the bridge is necessary or it can be replaced by the sp^3 hybridization, some of the synthesized isocombretastatins were reduced. The activity of phenstatins is really reduced in the diarylmethanols.

By standard catalytic hydrogenations, the expected products **48** and **63** were obtained. The reduction also affects other groups present, such as the formyl (**52**) and the nitro groups (**26**, **27**) (figure 29).

III.1.B. <u>Synthesis of phenstatin derivatives with heterocycles other than indole</u>.

Another planned objective of this work was the replacement of the 5-inolyl system by other heterocyclic moieties. Due to their similarity, structurally related benzofused pentagonal heterocycles were selected. The synthesis of phenstatins containing the 3,4,5-trimethoxyphenyl moiety and 1,3-benzoxazole or benzimidazole moieties were planned, according to the procedure depicted in scheme 3.

III.1.B.1. Starting materials.

The following procedures were used for the preparation of commercially unavailable starting materials,

<u>Synthesis of benzimidazoles **14** and **15**</u>.

N-methyl-5 and 6-bromobenzimidazoles (**14 and 15)** were prepared by treatment of 5-bromophenylene-1,2- diamine with methyl orthoformate, followed by phase transfer alkylation of the nitrogen atom (Figure 30). A mixture of regioisomers was produced, and used without separation because they proved to be irresolvable. The mixture, although non desirable, is useful to test the activity of any of its components, whose isolation could afterwards be undertaken, if considered necessary.

<u>Synthesis of 5-bromo-1,3-benzoxazole (**17**)</u>.

The synthesis of this starting material was completed by the same reaction using 4-bromo-2-nitrophenol and methyl orthoformate, using the required aminophenol (Figure 31).

III.1.B.2. Synthesis of diarylmethanols.

The same methodologies used for the preparation of indolefenstatins were used for the synthesis of the diarylmethanols carrying the benzimidazole and benzoxazole moieties,

Synthesis of compounds **69** and **70**.

After the treatment of the mixture of 5and 6-bromo-1-methylbenzimidazoles with two mmol of *n*BuLi /mmol and one mmol per mmol of 3,4,5-trimethoxybenzaldehyde, the resulting diarylmethanols were bonded through position 2 of the benzimidazole system. The products kept the bromo on the benzimidazole.

These compounds could be separated by chromatography, and identified (Figure 32) by comparison with the ketones produced by oxidation, which were characterized by means of nOe studies.

Synthesis of compound **73**.

The benzoxazole derivative **73** was prepared following the same procedure. However, the diarylmethanol bonded by position 5 was the only product (figure 33).

III.1.B.3. Synthesis of phenstatins.

The phenstatins **71**, **72** and **74** carrying the benzofused heterocycles were prepared by PDC or $KMnO_4$ oxidations of the corresponding diarylmethanols, as described in the previous sections. A general deshielding of all aromatic protons was observed in their ^1H NMR spectra (table 4 and figure 34).

III.1.C. <u>Synthesis of combretastatin derivatives</u>.

With the aims of comparing some combretastatins with the phenstatins and isocombretastatins synthesized in this work, the preparation of some derivatives with the same combination of aromatic rings was undertaken. In this way, the 3,4,5-trimethoxyphenyl ring was chosen as ring A and the ring B was any of the *N*-methylindole-3-carbaldehyde, *N*-ethylindole-3-carbaldehyde, *N*-methylindole-3-methanol and *N*-methylbenzimidazole systems previously studied (Figure 35).

The syntheses were completed by the Wittig reaction (Scheme 4) between the ylide from (3,4,5-trimethoxybenzyl)triphenylmethylphosphonium bromide and the above cited aldehydes.

III.1.C.1. Starting materials.

The required aldehydes were obtained from commercially available materials by means of *N*-alkylation, formylation and other reactions.

<u>Synthesis of 1-methyl-1*H*-indole-5-carbaldehyde (**4**).</u>

The direct methylation of 1H-indole-5-carbaldehyde, produced this compound (Figure 36).

<u>Synthesis of 1-ethyl-1*H*-indole-3,5-dicarbaldehyde (**3**).</u>

To avoid the *Z,E*-isomerization of the combretastatins during the formylation reactions, the formyl group was previously introduced in the starting material. Following the methodology described in section III.1.A.5.2, the dialdehyde was obtained in low yield, due to undesired polymerization reactions. Later, the absence of isomerizations during the formylation of combretastatins was stated and the formylation of these products was carried out after the Wittig reaction. Consecutive formylation and alkylation reactions yielded dialdehyde **3** (Figure 37).

<u>Synthesis of benzimidazole carbaldehydes **7** y **8**.</u>

Their synthesis was started from benzimidazole-5-carboxylic acid. *N*-alkylation reaction on the free carboxylic acid was rejected due to solubility problems (high water solubility), as well as on the binzimidazole-5-methanol, where *O*-methylation was also produced.

In consequence, reduction of the carboxylic acid to alcohol followed by MnO_2 oxidation produced benzimidazole-5-carbaldehyde, which was alkylated by the phase transfer catalyst methodology. By this procedure, the mixture of both *N*-methylation regioisomers **7** and **8** was achieved, along with a product of cleavage of the imidazole ring (**9**) (figure 38).

III.1.C.2. Synthesis of combretastatins analogues.

The combretastatins analogues were obtained by the standard Wittig methodology. Reaction products were isolated by means of chromatography and the *Z* and *E* isomers characterized according to the following differences: 1) chemical shift of olefinic protons of the *trans* (7.0 ppm) larger than the *cis* (6.7 ppm) isomers, 2) coupling constants of the olefinic protons larger for the *trans* (16 Hz) than for the *cis* (12 Hz) isomers, and 3) shielding of 2,6-protons and 3,5-methoxy groups in the *cis* isomers, due to the ring current effect of the other aryl group, in comparison with the unshielded *trans* isomers.

<u>Synthesis of 1*H*-indole-3-carbaldehyde **75**.</u>

For the synthesis of this compound the order of the addition was reversed to have a defect of the ylide in comparison to the dialdehyde, to ensure the reaction of the more reactive 5-carbaldehyde and to prevent the double reaction yielding triaryl derivatives (Figure 39).

After purification, the yield was only 5% and the synthesis was changed to use formylation of the preformed combretastatin as the last step.

Synthesis of benzimidazole derivatives **79** and **80**.

As expected, the use of the mixture of 1-methyl-1*H*-benzimidazole-5and 6-carbaldehydes in the Wittig reaction, produced a mixture of four isomers (Figure 40).

Synthesis of indole derivatives **76*Z*** and **76*E***.

The known indole combretastatins **76** were also synthesized with the purpose of preparing the formylated derivatives and comparing formylated and unformylated derivatives (Figure 41).

Synthesis of derivatives **77** and **78**.

According to previously described methodologies for isocombretastatins, the formyl derivative **77** and the methanol derivative **78** of the *N*-methyl-indolecombretastatin were prepared (Figure 42).

III.2. SYNTHESIS OF MACROCYCLIC COMPOUNDS.

The synthetic part of this work was completed with the preparation of two families of macrocyclic compounds related to combretastatins, containing a spacer between both aromatic rings in order to maintain the *cisoid* disposition.

In previous work from our group, several macrocyclic combretastatins, carrying phenyl rings substituted with methoxy or hydroxy groups and bonded through *para-para* or *para-meta* positions, were synthesized (Figure 43). In general, they show a diminished antimitotic activity, being more active those bonded between the two *para* positions through a hexamethylene spacer.

In this work, we decided to maintain the *para-para* connection, but introducing a greater conformational restriction by the presence of an indole system. Taking into consideration that molecular modelling suggest that methylene groups of the spacer can occupy the position in tubulina of one methoxy group of colchicine, mono- or di-methoxyphenyl rings were used (Figure 44).

The McMurry coupling was selected for the synthesis of these macrocycles, because it was useful to obtain previous members of these families, whereasGrubbs methatesis failed to produce them.

The synthetic plan is illustrated in figure 45. Two consecutive alkylation reactions, starting from indole-5-carbaldehyde, produce the dialdehydic intermediate to be used in the macrocyclization reaction.

III.2.A. <u>Monoarylic and diarylic intermediates</u>.

Using aldehydes depicted in figure 46 and 1,6-dibromohexane as alkylating agent, an initial alkylation (figure 47) by the phase transfer catalyst methodology followed by an alkylation using carbonate in DMF, produced dialdehydes **82** and **83** in high yields (figure 48).

III.2.B. <u>Macrocyclic compounds</u>.

McMurry reaction produces macrocyclizations yielding olefins or pinacols depending on the temperature. Whereas pinacols are obtained at lower temperature, olefins predominate at reflux.

The reaction was carried out in two consecutive steps, as follows: 20 mmol of $TiCl_4$ and 10 mmol of Zn (per mmol of dialdehyde) were mixed in THF at 0 ºC, then the dialdehyde (**82** or **83**) was added and the reaction refluxed for 5 h. Following this methodology, compounds (**84-89**) shown in figure 49 and yields in table 5, were produced.

The *cis* and *trans* diols were independently acetylated in order to modify their volume, hydrophobic character, solubility and hydrogen bonding capacity, while maintained similar spatial disposition; in order to check the effect of the acetates on the antimitotic activity. Diacetates **90-93** can also provide information for the spectroscopic and spatial disposition assignment of these compounds (figure 50).

III.3. SPECTROSCOPIC ANALYSIS OF MACROCYCLIC COMPOUNDS.

The structural determination of these compounds (**84-93**) was carried out by ^{1}H and ^{13}C-NMR studies and X-ray diffraction of compound **87** crystals.

III.3.A. <u>Olefins</u>.

Olefins **84** and **87** show a single set of signals, with a unique signal for pairs o groups of chemically equivalent nuclei. The ^{1}H-NMR data are shown in table 6, along with the characteristic coupling constant for *cis* double bonds($J \approx 10$Hz). There is an appreciable broadening of the signals of tetrasubstituted phenyl ring. This fact might be attributed to a change in the mobility of the macrocycle.

Olefin **87** is crystalline, so that its conformation in the solid state was established by X-ray diffraction (figure 51).

III.3.B. <u>Diols and acetates</u>.

In previous work from our group, it was established that the spectroscopic characteristics of bridge methynes of diols and acetates, facilitate their stereochemical assignment, as summarized in table 7.

Following these rules, the relative stereochemistries of diols and acetates were deduced as shown in table 8 for compounds **85-93**.

In short:

- Coupling constants for methyne protons are $J > 7.5$ Hz for *trans* and $J < 5.0$ Hz for *cis* stereoisomers.

- Average chemical shifts of methyne protons of the bridge are > 5.2 ppm in diols and > 6.2 ppm in diacetates for the *cis*, and < 4.7 ppm in diols and < 6.2 ppm in diacetates for the *trans* stereoisomers.

- Average chemical shifts of oxygenated carbons of the bridge (diols or diactates) are < 77.5 ppm for the *cis*, and > 79.5 ppm for the *trans* stereoisomers.

Other previously observed differences for the *cis* and *trans* stereoisomers are the chemical shift differences for the methyne protons and methoxy groups on tetrasubstituted rings (derived from syringaldehyde), that are summarized in table 9. In the present work, such a difference is not observed between *cis* and *trans* stereoisomers, a fact that can be attributed to the conformational restrictions introduced by the indole nucleus. The differences actually observed are shown in table 10.

III.4. CONFORMATIONAL ANALYSIS OF MACROCYCLIC COMPOUNDS.

As discussed, the macrocyclic derivatives were planned to block the *cisoid* disposition of the two aromatic rings. This macrocyclization produces a restriction of the mobility, translated into appreciable differences in the NMR spectra. To analyze these differences, these compounds have been grouped according to the bridge structure: olefins, *trans* diols and *cis* diols. In forthcoming sections, the following aspects will be discussed: 1) "a priori" analysis of conformations that can be adopted in each case, 2) theoretical studies, by means of molecular mechanics and dynamics of the accessible conformations, and 3) justification of the appearance of the NMR spectra.

Up to now, three generations of *para-para* macrocyclic analogues of combretastatins have been obtained. The first generation contained two symmetric (one disubstituted and other tetrasubstituted) phenyl rings (compounds **0B**, **0C**); the second generation enclosed by compounds with one symmetric (disubstituted or tetrasubstituted) and one asymmetric rings (compounds **0A**, **0D**, **0E**, **0F**). The third generation, formed by the compounds synthesized in this work, contains an indole system (see figure 51).

III.4.A. <u>Olefins</u>.

III.4.A.1. Analysis of conformations.

Symmetric macrocyclic olefins show NMR spectra with only one set of signals. A simple change of the helicity averages magnetic environment of chemically equivalent nuclei. Spectra of olefins with one asymmetric ring (**0D-0F**) also show a single set of signals, not explainable by just the helicity change.

In order to have a deeper understanding of the conformational possibilities, different equilibriums were analyzed. For stilbenes, two helical dispositions are possible (+ and -. Figure 52 top and bottom), which could be interconverted by either one ring rotation (Figure 52, on the left, ring D rotation and ring I *flip*) or a *double flip* process (Figure 52, on the rigth). A *flip* occurs when the plane of the ring passes through the perpendicular of the double bond (substituents on the ring are maintained at the same side of the double bond, for example marked positions of the I ring on the left or both marked positions on rings I and D on the right, figure 52). A ring rotation takes place when the plane of the ring passes through the plane of the double bond (substituents on the ring change from one side of the double bond to the other, for example marked position of the D ring on the left). In figure 52 a schematic representation is included, where the double bond correspond to the horizontal line and the aromatic rings with the vertical (or oblique) lines.

Conformational possibilities of macrocyclic combretastatins result from changes in the helicity (+ and -), substituent disposition for ring I (left ring) (above and below the double bond plane) and substituent disposition for ring D (right ring), thus resulting in 8 basic conformations as depicted in figures 53-58. They have been named **+I** to **+IV** and **–I** to **–IV**, depending on the helical sign of each one. When symmetric rings are involved, several possibilities become identical, although marked positions are situated above and below the double bond plane.

The conformational exchange between these eigth posibilities, can happen by any of the following processes (Ring I is now called T- from <u>Tri</u>-substituted-ring, and ring D is now called D or Q, from <u>Di</u>-substituted or <u>Tetra</u>-substituted rings), as shown in figure 53:

a)   T ring rotation (accompanied by ring D *flip*), occur along the horizontal.

b)   D or Q ring rotation (accompanied by ring T *flip*), take place on vertical exchanges.

c)   *double flip* processes, occur obliquely.

All these processes change the helicity, although only the *doubl*e *flip* occurs without passing a ring plane through the intrannular space.

<u>Conformational equilibrium for macrocyclic olefins with two symmetric phenyl rings.</u>

In order to help in the analysis of the dynamics behaviour of the macrocyclic indoles, the situation for the previously synthesized macrocycles **0D-0F** will be considered. First of all, compound **0F** with one disubstituted symmetric ring and one trisubstituted ring will be discussed, followed by more constrained situations: **0E** (smaller 3-oxapentamethylene spacer and intra-annular space) and **0D** (methoxy substituents on the symmetric Q-ring).

In order to explain spectra with a single set of signals and common signals for the chemically equivalent positions, three fast movements a), b) and c) can be considered, or at least two of them (see table 12 and figure 53). If only one is fast on the NMR time scale, two set of signals (Table 11, left column, fast T-ring rotation) or different signals for the chemically equivalent positions (for example dot and empty circle, table 11. Center, fast D-ring rotation, and right, fast *double flip*, columns) would have to be observed.

If any two of three movements were fast, the spectra could also be explained, because one set of signals with unique signals for chemically equivalent positions will observed, due to a rapid exchange between four conformational possibilities which include every possible kind (+I, -II, +III and –IV and –I, +II, -III and +IV) (Table 12 and figure 53).

Olefinic macrocycles with one symmetric and one asymmetric phenyl ring. Conformational equilibria for **0D**, **0E** and **0F**.

The four conformations in the upper part of figure 54 for compound **0F** are identical to the four conformations in the lower part (only identical marked positions change), and those on the left are mirror images of those on the right. To explain the NMR spectra of **0F**, at least two movements must be fast in order to interchange *endo*-MeO and *exo*-MeO dispositions and produce only one signal for chemically equivalent positions. These movements have been depicted in figure 54, although those requiring the pass of the larger methoxy group through the intra-annular space are not shown.

When the intra-annular space is reduced from eighteen to seventeen atoms (**0E**, figure 55), the signals of symmetric D ring are broadened. This fact requires that only one movement is fast (the other two slow or intermediate in the NMR time scale).

For the more hindered compound **0D**, one single set of signals and single signal for chemically equivalent positions are observed. Although four conformations in the upper part (figure 56) are identical to those in the lower part, two movements must be fast to explain the spectra. That requires the fast rotation of T-ring, in order to exchange chemically equivalent positions (for example red –OMe and black –OMe). Also *double flip* must be fast in order to interchange *endo*-OH and *exo*-OH conformations (unless one of them was more stable). Q-Ring rotation must be forbidden because it requires the pass of one bulky MeO- substituent through the intra-annular space. Fast *double flip* by itself would not explain the spectra, as it would not exchange the MeO- groups (or the aromatic methynes of the tetrasubstituted ring) from the same to the opposite side of the hydroxyl group.

In consequence, the reduction of the intra-annular space from eighteen to seventeen atoms is responsible for slowing down the interconversion of conformations involved in the equilibrium.

<u>Macrocyclic olefins with an indolyl moiety. Conformational analysis of **84** and **87**.</u>

Compound **87** can be considered analogous to **0D** with a more rigid indole ring instead of the trisubstituted ring, whereas compound **84** is a less symmetric variant. Eight conformational possibilities for each compound are depicted in figures 57 and 58, with the equilibriums between them (lightened arrows indicate less probable rotations, because they require the pass of a methoxy group through the intra-annular space, in vertical, or an unattainable elongation of the spacer, in horizontal).

III.4.A.2. Molecular mechanics and dynamics studies of olefins 84 and 87.

<u>Molecular mechanics.</u>

Because of the rigidity introduced by the indole system, several of the conformations represented in figures 57 and 58 would have no to be taken into consideration. For example, those conformations with the *N*-spacer bond in the *exo* disposition (±II and ±IV) seem to be less stable. To know the more accessible conformations for compounds **84** and **87**, conformational searches (Monte Carlo) using molecular mechanics (MM3 force field using chloroform as solvent) were carried out.

For each conformation found, two dihedral angles, DI and DT, were measured. Their values were used to assign the conformation groups ±I-±IV (as depicted in figure 59 c and d). To avoid potential differences arising from losses of ring planarity, observed during molecular dynamics, the values of each angle and its complementary were accounted for in the calculations.

The helical sign for each aromatic ring disposition was established as depicted in figure 60. If the sign of both dihedral angles is coincident, the conformation is assigned that sign. If not, the conformation was marked as non coincident with the defined groups. Conformations **+I** to **–IV** are included in table 13, with the range of dihedral angles values (columns 2 and 4) and schematic representations of each conformation (columns 3 and 5).

Conformations not belonging to classes ±I-±IV are grouped according to table 14. Those conformations with an angle in the interval ±10º close to a category change (*flip* for angles close to +90º or -90º, *rotation* for angles close to ±0º or ±180º) are included. In table 14 the intervals are in the first column, examples of each type in the second and indicative names in the third.

These rules were applied to conformational searches results for compounds **84** and **87**, allowing us to assign and analyze the conformations. Conformations **+I** to **–IV** are indicated by horizontal lines (-IV,+III,-II,+I,-I,+II,-III,+IV form above to below) , and those not classified (according to table 14) are represented by coloured horizontals (*double flip* –blue-, ring-D rotation –orange-, *double flip* –blue-, ring-I rotation –green-, *double flip* –blue-, ring-D rotation –orange-, *double flip* –blue-; from above to below), of increasing energy from left to right.

Results are also presented in table 15. For each compound, the minimum energy conformations found after 1000 rounds are included, showing in the upper part the energy difference with respect to the global minimum (shadowed cell) and the times found in the lower part (into brackets).

Energy differences between identical conformations inform on the intrinsic error of the method, originated by: used force fields or difficulty to find a minimum from strained conformations.

The conformations of minimum energy found for compound **84** are of type I and III, whereas conformations of types II and IV are less populated. In the case of compound **87**, there are small differences in energy between all conformations, I=II and II=IV, and all of them have to be taken into account. The structure of compound **87**, obtained by X-ray diffraction correspond to –I/-III, as shown in figure 63.

In compounds **84**, **87** and **0D-F** conformations other than I-IV are observed, whisch are classified in the double *flip* category.

Molecular dynamics.

In order to study the transicions between conformations for compounds **84** and **87**, molecular dynamics studies have been carried out. Simulations for 3 ns at different temperatures (300, 600, 1200 and 1500 K), were performed using the same conditions described for Monte Carlo conformational searches. Analogous simulations were conducted with model structures lacking the spacer in order to assist in the analysis of the results.

The results of the molecular dynamics were analyzed in the same way as the conformational searches, by clasifying conformations as type ±I to ±IV and those corresponding to transitions between them. Each conformation was compared with the following one in the simulation to analyze how the transitions take place. For instance, a transit from +III to –I is assigned to a indole ring rotation –IRot-. As temperature raises, the number of conformations different than type ±I to ±IV increases notably.

Because processes responsible of the aspect of NMR spectra take place in the micro seconds, they are inaccessible to these simulations, but molecular dynamics picture a panoramic on the relative ease of these processes. The temperature of simulations was increased in order to facilitate the surrounding of energy barriers, thus processes which are unattainable at lower temperature can be observed at 1500 K.

Molecular dynamics simulations at 300 K for non-macrocyclic analogues (**0H** and **0G**, figures 64a,b) of compounds **84** and **87** show that all conformations are accessible, with positive and negative helicities.

Figures 64a and 64b summarize the results of the molecular dynamics simulations (MD) for **0G** and **0H** at 300 K (top) and 1200 K (bottom). Conformations ±I to ±IV and intermediate situations (IRot, DRot, TRot, *double flips*) are indicated on the ordinate axes. Centre of figure: Transitions assigned to exchanges observed during the simulation at 300 K, with transitions (no transition =, *double flip* DF, ring rotation IRot or RRot, with transition states below them) for indole and phenyl ring in purple and blue respectively, and overall transition in red (= means no change, RRot means that one ring rotates and the other *flips,* DF means a *double flip,* points below indicate a transition state for the category above and ++ means complex transitions). The same applies for the following MD graphs.

Structure **0G** shows a preference for conformations type III, being I and IV also well represented, and conformations type II are less frequent (figure 64a). As shown in table 16, there is a preference for the methoxy group to adopt an *endo* disposition, being the disposition of the indole moiety less important. Conformations II, with *endo* methoxy and indole are greatly disfavoured.

In the case of **0H**, type I and III are the same, as well as type II and IV, the former two predominating over the later (figure 64b). The indole preference for an *exo* disposition (or the repulsion exerted by a perennial *endo* methoxy) becomes the dominant factor when there is always an *endo* and *ex*o methoxy group.

At 1200 K the residence time in each conformation is lower, facilitating the occupation of all conformational types. Both compounds have a similar behaviour at this temperature. Rotations of all the rings are observed, including indole, tri- and tetra-substituted ring rotations and *double flips*. Apparently, **0H** has greater difficulty to complete rotations of the indole system (changes between lower and upper part of diagram A).

Molecular dynamics of compounds **84** and **87** at 300 K and 1500 K (Figure 66 a and b), show only conformations type –I and +II, altogether with *double flips*, which represent their intermediate situation. This fact clearly illustrates that the spacer reduces the conformational flexibility of these compounds, allowing only the *double flip* to easily take place.

When analyzed at the same temperature, the results for compound **87** (Figure 66b) show higher mobility than compound **84** (figure 66a). This *double flip* facilitation by the presence of two methoxy groups in **87**, and can be explained by a destabilization of ground state type -I conformations, due to interaction of the *endo* methoxy with the spacer, (figure 65 on the left, red colour) with respect to the transition state (figure 65 on the rigth), where the two methoxy groups point outwards. In comparison, the ground state for compound **84** displays lower interactions between the methoxy and the spacer and the energy barrier is thus higher (Figure 65, green arrows).

In order to discriminate between spacer effects and those due to rigidity introduced in the system by the indole ring, molecular dynamics for **0D**, **0E** and **0F** were also carried out.

Compounds **0D** and **0E**, with a longer hexamethylene spacer, show identical results. Accordingly, MD results for only one of them (**0F**) and for **0E**, with a shorter 3-oxapentamethylene spacer, are presented in figures 67 (300 K dynamics, 300 K transitions of **0E** -67a- and **0F** -67c-, and 1200 K dynamics and 1200 K transitions of **0E** -67b- and **0F** -67d-). At 300 K, only major conformation type ±III and minor one type ±IV, along with the intermediate *double flip* between them, are observed. At 1200 K, only these transitions become more frequent. Also, a trisubstituted ring rotation occurred for compound **0F**, with a longer spacer and larger intra-annular space. This rotation gives way to conformations type –I and +II. In order to better show the rotation, dihedral values, analogous to DI and DT, have been plotted for each conformation along the MD simulation of **0F** and **0E** in figure 68. The upper traces correspond to the dihedral of the disubstituted ring and the upper ones to the trisubstituted one.

We have previously shown that the related glycol **0J**, with a shorter spacer, does not rotate any ring at 1200 K, but **0K**, with a longer spacer, rotates the disubstituted ring. It The preference of compound **0F** for rotating the trisubstitued ring in the presence of a disubstituted ring was initially surprising. For **0K** rotation of the disubstituted ring is the only option, as rotation of the Q-ring requires (passing one methoxy group through the intra-annular space.

As mentioned, for compound **0F**, both rings can rotate passing hydrogen atoms through the intra-annular space. However, rotation of the trisubstituted ring put further away the methoxy group (diminishing the interaction with the spacer, figure 69 right) in comparison with starting conformation (on the left), whereas the rotation of the disubstituted ring brings the methoxy group closer to the spacer and the rotating disubstituted ring (figure 69, centre).

All these results agree with the MD simulations for **84** and **87**, which show no rotations of rings due to the increased rigidity. Conformations with the indole ring almost coplanar with the double bonds are observed, as well as a lower mobility of the trisubstituted compound **84** in comparison with the tetrasubstituted compound **87**. An explanation for this difference is given in figure 65, where the transition state for the *double flip* is shown on the right and the ground state conformations on the left. The methoxy groups of the Q-ring interact with the spacer and destabilize the ground state, thus making the transition easier. Indole derivatives, due to the rigidity introduced in the system by the indole moiety, are expected to be less mobile than phenyl exclusive macrocycles.

III.4.A.3. Discussion of NMR spectra of olefins 84 and 87.

All the macrocyclic olefins here described show NMR spectra with single sets of signals, except **0E** and **87**, which show broadened signals for exchangeable positions. That requires that two fast rotations on the NMR time scale, being one the *double flip*. Molecular dynamics simulations gives an idea of the difficulty for ring rotations, which are always slower than *double flips*.

Fast *double flip* and slow-intermediate indole ring rotation (passing hydrogen atoms H-5 and H-6 through the intra-annular space) could explain both spectra. For compound **87** intermediate rotation of the indole is responsible of the line broadening, while *double flip* averages ±I/±III with ±II/±IV. The same type of processes in compound **84** would lead to two sets of signals, one for the ±I/±II ensemble and the other for ±III/±IV. Either rotation of the disubstituted is fast, in disagreement with the MD simulations, or one ensemble is not being seen (due to a lower stability).

These conclusions are summarized in table 17.

III.4.B. Diols and diacetates.

III.4.B.1. Analysis of conformations.

<u>Analysis of conformations of diols with two phenyl moieties</u>.

Diols show a higher conformational freedom than olefins, due to the possibility of bridge rotation. The possibilities depicted in figure 70 can be taken into consideration for the conformational analysis: a) A-ring rotation, green arrow, b) B-ring rotation, orange arrow, c) bridge rotation, changing between the two *synclinal* dispositions for the two aryl moieties, grey arrow, and d) change of helicity of both rings (signs of dihedral angles defined by the planes of the rings and the central bond of the bridge), blue arrow. Bridge rotation and helicity changes have no severe limitations, because they do not require the pass of substituents through the intra-annular space.

These four possibilities lead to sixteen reference conformations, shown in figure 71 (each one has a different combination of bridge disposition –SC (+ or -)-, helicity -(+ or -)-, T-ring rotation – *exo*/*endo* disposition of substituents- and D/Q-ring rotation – *exo*/*endo* disposition of substituents-). Sixteen conformations are connected in figure 72 by arrows showing the conformational change required for passing from one to another. Groups **A**, **B**, **C** and **D** of related conformations are formed by those produced by easier changes, helicity and bridge rotation, that can take place independently or simultaneously.

According to previous work, preferred conformations of *trans* diols are those depicted in the centre of figure 72 (I-VIII), with a *gauche* disposition of both hydroxyl groups. In the case of *cis* diols, both possibilities for bridge rotation must be similar, because they all have *gauche* dispositions for the hydroxyl groups. A simplified picture of these bridge rotation equilibria is depicted in figure 73.

The study of diols and diacetates with two phenyl moieties has been carried out in previous work. In short, NMR spectra show one or two sets of signals, all of them having different signals for the chemically equivalent nuclei. Two sets of signals indicate two conformations in slow equilibrium, while one set indicates the existence of a preferred conformation or a fast equilibrium. Broadening of signals can be attributed to intermediate exchanges on the NMR time scale.

<u>Analysis of conformations of diols with one indolyl moiety.</u>

As explained in the previous section, sixteen base conformations I-XVI can be considered for diols **86** and **89** and their diacetates **91** and **93**. These conformations and the conformational changes passing from one to another are shown in figures 74a,b (conformations for **86** and **89**), figures 75a,b (conformational changes for **86** and **89**), figure 76 (**85** and **88** conformations) and figure 77 (conformational changes for **85** and **88**).

III.4.B.2. Molecular mechanics and dynamics of diols and diacetates.

In order to know the more stable conformations, to take into consideration for conformational discussions, conformational searches (Monte Carlo) with molecular mechanics (MM3 force field, chloroform as solvent) and molecular dynamics simulations at different temperatures (300K and 1200K) were carried out.

In order to assign each found conformation to conformational groups I-XVI, three dihedral angles were measured (Figure 78). They correspond to bridge rotation (grey), indole ring rotation (green) and phenyl group rotation (blue). The atoms defining the dihedral angles are indicated by orange circles.

The conformations were assigned to the dispositions + and – *synclinal* by using the values of the dihedrals of the central bridge bond (DP), defined as shown in figure 78. This definition renders the values independently of the absolute and relative stereochemistry of diols. For ring rotations, dihedral angles DI (green) and DT or DQ (blue) were defined as shown in figure 78 (bold bonds and orange circles). As for olefins, marked dihedral angles and the complementaries of the alternative dihedral completed by the smaller orange circle, were measured and averaged.

Once the dihedral angles were measured, +*SC* and –*SC* conformations were assigned. The sign of the bridge dihedral angle (DP), allowed us to distinguish between I-VIII (-*SC*) and IX-XVI (+*SC*). Accordingly, they will be depicted in the negative and positive parts of ordinates axis in forthcoming figures. Dihedral angles for indole and phenyl rings define *endo*/*exo* dispositions and the helicity sign, according to conformational groups shown in table 18. The *endo*/*exo* definition for dispositions of substituents was as depicted in figure 79, *endo* when the substituent is located between both rings. In the absence of other changes, the pass from –*SC* to +*SC* conformations (and *vice versa*), also changes the *exo* and *endo* disposition of substituents.

The helical sense for each ring was defined by the angle formed between that ring plane and the plane defined by carbons of the bridge and the aromatic carbon bonded to them (Figure 80). Dihedral angles $\theta > 90º$ and $0 > \theta > -90º$ were assigned negative helical sign (-). If the signs for both rings were coincident, that sign was assigned to the helicity. On the contrary, if the signs were not coincident, the conformation was marked as no corresponding to those initially considered (I-XVI). In graphics showed in figure 84 and following, conformations with discordant helicities were indicated by brown positions in the horizontal marked with Hel≠ symbol.

In order to get a better picture of the fine disposition of the aromatic rings, their relative disposition respect to the substituents on the benzylic carbon were analyzed. The circumferences defined by the rotation of the ring plane were divided into three thirds by the substituents, and designed C-H, C-OH and H-OH. The situation of the ring is defined according to figure 81. When the plane of the ring is close (±10º) to a substituent (being the bond of the ring eclipsed on the side closer to the first substituent of the ring), it is indicated in red (green if it is the opposite side). When the plane of the ring is close to the C-C bond, a ring rotation is produced (indicated in purple).

<u>Analysis of molecular mechanics results</u>.

Following the aforementioned criteria, conformations found during the conformational search for compounds **85**, **86**, **88** and **89** have been classified within the I-XVI categories (figures 82a-d). Table 19 summarizes the relative energies of the conformations representing the local minimum for each conformational class with respect to the global minimum (indicated by shadowed cells). Compounds with the same relative stereochemistry behave quite similarly. *cis* and *trans* compounds mainly differ in the number of synclinal dispositions they adopt. *cis* compounds populate both synclinal dispositions whereas *trans* ones mainly adopt the one with gauche hydroxyls. The energy difference between conformations is not high, and every conformation has to be taken in account. For diols **86** and **89**, with symmetrical phenyl ring, conformation I is identical to conformation III, V is equal to VII, X to XII and XIV to XVI. The energy differences calculated between them are smaller (less than 0.7 kcal/mol) than those found for olefins, suggesting a more flexible behaviour.

In every case, conformations with a plus synclinal disposition +*SC* (**I-XVI**) are more stable if the phenyl rings adopt a positive helical twist (**X**, **XII**, **XIV** and **XVI**) and negative synclinal dispositions –*SC* (**I-VIII**) prefer negative helical twists (**I**, **III**, **V** and **VII**) indicating an energetic coupling of both descriptors. As shown in figure 83, the more stable combinations place the phenyl rings so that they leave more room in the intra-annular space for the spacer (larger ellipsoids in the centre of figure 83).

Detailed analysis of the observed conformations is shown in figure 84a for *cis* diols **85** (upper) and **88** (lower) and 84b for *trans* diols. Trisubstituted phenyls and indole rings adopt both *endo* and *exo* dispositions. However, in compounds with tetrasubstituted phenyl rings (which always place one methoxy group *endo*) the indole ring is preferently *exo*, suggesting an energy penalty for conformations with both substituents *endo*, as previously suggested for the olefins. In most of the stable conformers, both phenyl rings show the same helical sign. The observed dihedrals for the phenyl rings (green lines) show a preference for conformations in which the ring planes are close to perpendicular to the plane joining them, placing them away from the intra-annular space.

Analysis of molecular dynamics simulations.

Molecular dynamics simulations have been carried out at 300 K and 1200 K in order to explore the transitions between conformational classes, and the results were analyzed in the same way as the Monte Carlo searches (Fig 85a shows the conformations observed along the trajectories for the *cis* diols and 85b for the *trans* ones and Table 20 summarizes the conformations observed during the Monte Carlos and the molecular dynamics simulations). All the simulations started with conformation type X, except for **89**, which started with a conformation of type VII (absolute stereochemistry opposite to **86**). The comparison of two consecutive points along the trajectories allowed us to analyze the possible transitions (bridge disposition +*SC* or –*SC,* phenyl and indolyl rings rotations according to figures 80 and 81) and their relative frequencies.

At higher temperatures, more conformational classes and transitions were observed, as well as more conformations belonging to structural classes different from I-XVI (indicated by the zero value in the graphs). The simulations yielded similar results for compounds with tri- and tetrasubstituted rings. The most accessed conformations belong to structural classes I-XVI. Conformations with opposite signs for the synclinal disposition and the helical sense (less stable according to the Monte Carlo) are less populated than those with same signs, but they are easily accessed, suggesting a low energy barrier between them. These transitions (i.e. going from XII to XV and *vice versa*, or from VII to IV for **89**) are the only ones observed at 300 K.

At 1200K, new transitions occur, as shown in figures 86 and 87 (closer look at figure 85b): at 1200K, the most observed transitions are bridge rotations usually accompanied by helical sense changes (green arrows), and when not (purple arrows) are quickly followed by ring helical sense adjustments (red arrows). In fact, all of them are the same process, as helical sign changes are fast (they are not seen due to the different energy of conformations with matched and unmatched signs for SC and helical sense, as evidenced by the different occupation of XII and XV in figure 86). The easiness of these two transitions allows us to group the conformational classes in four groups: **A** (I-VI-X-XII), **B** (XVI-XI-VII-IV), **C** (XII-XV-III-VII) and **D** (XIV-IX-V-II) that have been anticipated in figures 75 and 77.

1200K simulations for *cis* diols also display some low frequency transitions: from XII to I for **85** (brown arrow in figure 86) and from III to V for **88** (brown arrow in figure 87). The first one implies a bridge rotation accompanied by a helical change (as usual) and by the unusual tri-substituted ring rotation (implying the cross of the phenyl ring plane by the plane defined by the bridge carbons and their bond to the considered phenyl ring, see figure 81). This transition allows for the exchange of the group of conformations **C** (XII-XV-III-VII) to **A** (I-VI-X-XII) as shown in figure 77. The second one implies the unusual rotation of the indole ring, allowing for the exchange between groups **C** (XII-XV-III-VII) and **D** (XIV-IX-V-II). The symmetrical nature of the tetrasubstituted ring in **88** makes **C** (XII-XV-III-VII) equal to **A** (I-VI-X-XII) and **B** (XVI-XI-VII-IV) equal to **D** (XIV-IX-V-II), so that all conformations are in fact sampled by the simulation. The low frequency of ring rotations does not allow to establish a relative order of feasibility for them, other than the difficulty of the tetra-substituted ring rotation, as it requires to pass one methoxy group through the constricted intra-annular space. No ring rotations were seen for *trans* diols.

The molecular dynamics simulations agree with the initial assumptions on the relative ease with which the different rotations occur and with their classification in four kinds: a) indole ring rotation, b) rotation of the phenyl ring, c) bridge rotation and d) helical sense change. Furthermore, a relative order of feasibility has been advanced: d > c > a ~b (tri-R) > b (tetra-R).

III.4.B.3. NMR spectra of diols and acetates.

III.4.B.3.a. <u>Fast bridge rotation-Interconversion of synclinal conformations.</u>

As previously indicated in the molecular dynamics section, if the d and c transitions between conformations are fast on the NMR time scale, the chemical equilibria accounting for the NMR spectra can be analyzed by considering the groups of conformations **A**, **B**, **C**, and **D** (figure 88 and figures 74 and 77). Within each group, *cis* diols mostly populate two conformations (e.g. conformations I and X for group **A**, as indicated in red), corresponding to the + and –SC conformations with matched helical sense sign for the rings, and can thus be represented by them. On the other hand, *trans* diols populate a single conformation within each group (corresponding to the one with gauche hydroxyls, and matched helical sense and synclinal disposition signs). Furthermore, for compounds with a symmetrical tetra-substituted ring (**86** and **89**), group **A** is equal to group **C** and group **B** equal to group **D**, so that only two groups have to be considered.

The chemical environment in which groups that behave differently in *cis* and *trans* diols (MeO-, aromatic ring protons and carbons) are found is indicated in figure 89 for compounds with a tri-substituted ring and in figure 90 for compounds with a tetra-substituted ring. Averaging of the situations within the group allows for a prediction of the averaged (or not) state for each substituent and can thus be applied to predict the signature of an NMR spectrum of each contributing group of conformations. Matching the expected data for each group of conformations to the found spectra will allow us to analyze the dynamics of each system.

According to the previous discussion, trans diol **89** (figure 91) should be the simplest system, with one symmetrical tetra-substituted ring (only two groups of conformations as **A=C** and **B=D**) and only one conformation contributes significantly to each group (i. e. I/III for **A/C** and V/VII for **B/D**). In any case, the chemically equivalent groups on the tetra-substituted phenyl ring are in different chemical environments in each group of conformations, so that we would expect different signals for each pair of them.

The NMR spectra for **89** show a single set of signals, with two signals for the chemically equivalent nuclei. A fast rotation of either the indole or the tetra-substituted (less likely) ring or of both of them, or a preference for one of the two groups of conformations (not predicted by the molecular mechanics calculations) must be invoked to explain the appearance of the spectra. The NMR spectra for *trans* diol **86** are very similar to those of **89**, suggesting a similar behaviour. In this particular case, either only one conformational group is preferred or both ring rotations are fast on the NMR time scale.

As discussed above, *cis* diols are more complex situations than *trans* ones, a prediction confirmed by their NMR spectra, which show at least two sets of signals and significant line broadening. This suggests that more complex conformational equilibria must account for the observations. For *cis* diols, two conformations must be considered within each conformational group (e.g. conformations I and X for group **A**), as shown for diol **88** (for which conformation **A** is equal to **C** and **B** equal to **D** due to the presence of a symmetric tetra-substituted ring) with red typeset in figure 92. In order to clarify the situation, the chemical shifts for chemically equivalent groups of nuclei which must be in different chemical environments according to their different behaviour are summarized in table 21. The large chemical shift difference between chemically equivalent methoxy groups and aromatic protons stands out. The fast chemical averaging within groups **A**, **B**, **C**, and **D** previously proposed should average them between *endo* (shielded by the ring current effect of the ring in front) and *exo* (not affected by the ring current effect). This observation suggests that bridge rotation is not occurring fast on the NMR time scale.

III.4.B.3.b. <u>Slow bridge rotation. Slow interconversion of synclinal conformations.</u>

An alternative explanation is thus proposed, in which rotation of the indole ring is fast, averaging conformations in new groups **E**, **F**, **G** and **H** (see also figure 96 for these groups in compound **89**), and bridge rotation is slow, as shown in figure 93. This explanation can easily be extended to *trans* diols, where the importance of the change is lessened due to the fact that bridge rotation in this case leads to unstable situations, already discarded. In order to explain the situation for **88**, the symmetrical nature of the tetra-substituted ring simplifies the analysis (as shown in figure 94). Again, **85** behaves quite similarly, and the considerations for the ring rotations would remain the same proposed for **86** and **89**.

Tis unified explanation, based on a slowred bridge rotation and, in some cases, faster T-ring rotation, is resumed in table 22. As shown, the expected situations match with the NMR spectra of synthesized macrocyclic diols and their diacetates.

III.5. BIOLOGICAL ACTIVITY.

III.5.A. <u>Tubulin polymerization inhibitory activity</u>.

III.5.A.1. Tubulin isolation.

Calf brain microtubule protein (MTP) was purified by two cycles of temperature-dependent assembly/disassembly, according to the method of Shelanski, modified as described in the literature (figure 97). The MTP solution was stored at -80 °C. Protein concentrations were determined by the Bradford's method, using BSA as standard. Six different MTP preparations were used in the tubulin assembly assays.

III.5.A.2. Tubulin assembly inhibitory activity of the compounds.

In vitro tubulin self-assembly was monitored turbidimetrically at 450 nm. The ligands were dissolved in DMSO and the final amount of DMSO in the assays was kept at 4%, which has been reported not to interfere with the assembly process. The increase in turbidity was followed simultaneously in a batch of six cuvettes (containing 1.0 mg/mL MTP in 0.1 M MES buffer, 1 mM EGTA, 1 mM $MgCl_2$, 1 mM β-ME, 1.5 mM GTP, pH 6.7, and the measured ligand concentration), with a control (i.e., with no ligand) always being included.

The samples were preincubated for 30 min at 20 °C in order to allow binding of the ligand, and were cooled on ice for 10 min. The cuvettes were then placed in the spectrophotometer at 4 °C. The assembly process was initiated by a shift in the temperature to 37 °C and the percent of inhibition (with respect to a sample with no drug) of tubulin polymerization at a single concentration (tipically 20 µM) was determined in at least two independent experiments for every compound. Compounds which inhibit tubulin polymerization more than 50% at 20 µM (predictable with IC_{50}s lower than 20 µM) were selected for the determination of their IC_{50}. The results are shown in table 23 for unselected compounds and in table 24 for selected ones.

III.5.A.3. Determination of the IC_{50} of tubulin assembly inhibitory activity of the selected compounds.

The IC_{50} was calculated as the concentration of drug causing 50% inhibition of polymerization after 20 min of incubation and was determined analytically. At least two independent experiments (or more when required) with different MTP preparations were carried out for each compound tested.

III.5.B. Cytotoxicity assays.

Cytotoxicity was measured against 4 cancer cell lines (HL-60, A-549, HeLa and HT-29) by Dr. Faustino Mollinedo (C.I.C. Centre for Cancer Research. University of Salamanca), using the XTT procedure, as published. The data are shown in table 26.

III.5.C. <u>Discussion of the results of biological activity</u>.

III.5.C.1. General considerations.

Macrocyclic analogues display low potency in TPI (tubulin polymerization inhibitory) activity and cytotoxicity assays. On the other hand, the rest of the synthesized compounds constitute a very potent family of cytotoxic and TPI compounds. A comparison of the result obtained in this work with previous works from our lab (figure 98) shows that this family constitutes a hotspot in chemical space for TPI activity. Accordingly, the combination of a trimethoxyphenyl ring with a *N*-methyl-5-indolyl moiety seems to be a quite favourable one.

Overall, there is a good correlation between TPI potency and cytotoxicity, as shown in figure 99 for average cytotoxicity against the four cell lines (blue diamonds) or either the maximal (yellow squares) or minimal (green triangles) cytotoxicity values obtained, suggesting that they are probably acting by inhibiting the polymerization of tubulin. The higher variability shown by the minimal cytotoxicity values possibly reflects the fact that resistance can arise from ways different from target differences, thus decreasing the sensitivity to some potent TPI compounds. When the different cell lines are compared (fig. 101: minus logarithm of cytotoxicity IC_{50} against each cell line vs the minus logarithm TPI IC_{50} values), HeLa and HL-60 seem to be more sensitive, whereas A-549 and HT-29 are more resistant.

The TPI assay at a single concentration seems to be an effective way of discarding candidates for further analysis and to focus on more interesting zones of chemical space. The TPI values at different concentrations of drug follow mono-exponential behaviours (figure 100), as expected. The IC_{50} measurements confirm the trends shown in the single concentration assays and allow for more precise SAR (structure activity relationships) analyses. Some of the IC_{50}s obtained in this work are amongst those of the most potent TPI compounds described up to date.

III.5.C.2. General structural considerations.

In order to compare the effect of different structural elements on the potency of the families studied we have compared the potencies of series of compounds having and lacking the structural feature under examination. Thus, we have compared series with 2,3,4- vs 3,4,5-trimethoxyphenyl rings, indoles vs substituted phenyls, and the bridges between aromatic rings (combretastatins vs phenstatins vs isocombretastatins) for otherwise identical pairs of compounds.

When a dispersion graph is represented in which the pairs of values are the –log (IC_{50}) TPI or cytotoxicities for compounds with a 2,3,4- (x axis) vs 3,4,5-trimethoxyphenyl ring (y axis), such as in figure 102, if both structural elements are equivalent the points are close to the diagonal. If the 2,3,4-trimethoxyphenyl renders the compounds more potent, the points sit mostly above the diagonal and if the opposite is true, the points sit mostly below the diagonal (as observed, indicating that the 3,4,5-trimethoxyphenyl is preferred). However, some compounds with a 2,3,4-trimethoxyphenyl group show acceptable IC_{50} values, an unexpected result if we consider previous results and literature data.

In order to further explore this observation, we have compared compounds with a 2,3,4-trimethoxyphenyl ring combined with either a substituted phenyl ring (blue diamonds and green bars in figure 103) with those with an indole ring (purple circles). To this end, we have plotted the TPI (bar diagram at the upper left) and the average cytotoxicity (bar diagram at the lower right) (figure 103). Purple circles aggregate at the upper right hand side, whereas the blue diamonds do so at the opposite end. This indicates a different behaviour for both types of compounds.

However, comparing simultaneously compounds with 2,3,4- or 3,4,5-trimethoxyphenyl rings differenciated by the presence of substituted phenyls or *N*-methyl-5-indolyl moieties as the other ring (figure 104), both classes are very similar, in agreement with previous reports which suggested that the *N*-methyl-5-indole moiety is a good surrogate for the 3-hydroxy-4-methoxyphenyl ring in combretastatins and phenstatins.

In figure 105 the average cytotoxicity values are plotted against the TPI values (both as –logs) for combretastatins (green triangles), phenstatins (pink diamonds) and isocombretastatins (yellow squares) in order to compare them. Phenstatins show lower cytotoxicities than the other two groups for a given TPI value, as indicated by their lower tendency line. As expected, hydrogenated compounds (blue stars) show low potencies, except compound **48**, indicated by an arrow on the graph.

III.5.C.3. Effects on the activity of structural elements.

As shown in figure 106, formil groups are very favourable in combretastatins, less so in isocombretastatins and not favourable in phenstatins. Hydroxymethyl derivatives are less potent (figure 107) than formilated ones, except in combretastatins. Also, an interesting increase in sensitivity of A-549 and HT-29 is observed in some cases. Other substitutions assayed (oximes, hydrazones and nitriles) lead to less potent compounds as shown in figure 108, where average potencies relative to unsubstituted compound **47** are represented, and in figure 109, where individual potencies relative to compound **47** are represented. The most favourable substituent is the nitrile, which, unlike others, combines well with 2,3,4-trimethoxyphenyl ring. It can also be seen in figure 109 that compounds of this class with a 2,3,4-trimethoxyphenyl ring are less potent against HT-29 (an often resistant cell line) and, perhaps more surprisingly, against HL-60. The nitrile substituted compound does not follow this trend. Oximes are also potent compounds.

The presence of an adicional formyl group at the bridge of isocombretastatins (figure 110) decreases the activity with respect to the monoformylated derivatives at the position C-3 of the indole system.

If we consider a pharmacophore model proposed for colchicine site inhibitors of tubulin polymerization, the indole ring can occupy three pharmacophoric sites (figure 112): a hydrophobic zone (black dots), a hydrogen bond acceptor zone (green dots) and a more distant hydrogen bond donor (pink dots).

The most favourable substituents found are thus small ones. When we attempted to dock the 3-substituted compounds in tubulin complexes with colchicine, the poses found were very different from those of compounds with unsubstituted indoles, suggesting that there is not enough room for the substituents in the model of the complex. Consistently, the dialdehydes **50** and **61** (structurally related also to ADAMs and CC-5079, see figure 110), are less potent than the parent hydrides. The replacement of the 3-CH of indole by a heteroatom also leads to low potency. A possible explanation for the good activity profiles observed for the 3-substituted indoles, despite of their reluctance to dock in the colchicine site might imply a different disposition of lysine 350β of tubulin (see figure 112), whose side chain might rotate generating some room for the derivatives, allowing at the same time for an interaction between the substituents and the amino group.

Macrocyclic combretastatins are neither active in TPI nor in cytotoxicity assays. Molecular modelling suggested that one of the methylenes of the linker might occupy the space that occupies one of the methoxy groups of colchicine when binding to tubulin. Accordingly, compounds lacking one of the methoxy groups where synthesized and assayed, and showed only slight improvements. Thus, it seems likely that the spacer is responsible for losing TPI activity. Docking studies on non-macrocyclic analogues suggest that the spacer might collide with the side chains of the residues forming β-sheet spanning residues 313Val-316Val and 348Asn-352Ala (figure 111).

As summary of the results obtained in this work it can be highlighted:

- Cytotoxic potency of isocombretastatins is comparable to that of combretastatins and both higher than phenstatins when the TPI activity is similar.

- 3,4,5-trimethoxyphenyl moiety leads to more potent compounds than the 2,3,4-trimethoxyphenyl ring, although for the last one the potency increases when combined with the *N*-methyl-5-indolyl moiety.

- The *N*-methyl-5-indolyl moiety moiety is also a good subrrogate of ring B in isocombretastatins, as it had been already observed for combretastatins and phenstatins.

- Other benzofused heterocycles, structurally close to indole, produce lack of activity.

- The presence of subtituents at position C-3 of *N*-methyl-5-indolyl moiety has a variable effect on the activities, being more potent those compounds with the nitrile or the oxime groups.

V. CONCLUSIONS

In this work it has been performed the synthesis and evaluation of new antimitotic agents related to combretastatins and phenstatins and, from the results, it is possible to infer the following conclusions:

1. The used synthetic methodology allows obtaining phenstatins, isocombretatatins and a large number of derivatives easily. These compound constitute a nex family of antimitotic agents.

2. It has been obtained dozens of compounds that combine a trimethoxyphenyl and an indol moiety through different bridges. The biological assay of these compounds allowed a direct comparison among combretastatins, phenstatins and isocombretastatins, which usually behave as highly potent agents in this assay and as cytotoxic agents when they carry group-rings.

3. Combretastatins and isocombretastatins show higher cytotoxicity than phenstatins when they have similar TPI potency.

4. The de *N*-methyl-5-indolil scaffold has proven to be a good replacement for the guaiacol moiety in isocombretastatins and as in combretastatins and phenstatins. On the contrary, other related heterocyclic rings, such as 1,3-benzoxazole and 1*H*-benzimidazole produce a decrease in the activity.

5. In general, compounds with a 3,4,5-trimethoxyphenyl ring are more potent than those with a 2,3,4-trimethoxyphenyl ring, but an increase in the potency it is observed when the 2,3,4- is combined with an indol moiety (in comparison to its combination with another phenyl moiety).

6. In isocombretastatins, the 3-substituted indole has no improved the activity respect the no-substituted indol. Nevertheless, the introduction of an oxime, a nitrile or a formyl group has produced compounds of similar potencies.

7. Following the methodology employed by our research group, two new families of macrocyclic combretastatins have been synthesized. Their conformational analysis completes the study about the mobility and the disposition of the rings of this restricted analogues.

8. It has been confirmed that the presence of an additional bridge (spacer), linking *para-para* positions of combretastatins and analogues, lead to total lack of tubulin polymerization inhibitory activity and cytotoxicity in these families of compounds.